

You might find this additional information useful...

This article cites 31 articles, 10 of which you can access free at:

<http://jn.physiology.org/cgi/content/full/79/4/1879#BIBL>

This article has been cited by 4 other HighWire hosted articles:

Stochastic Resonance in the Motor System: Effects of Noise on the Monosynaptic Reflex Pathway of the Cat Spinal Cord

L. Martinez, T. Perez, C. R. Mirasso and E. Manjarrez
J Neurophysiol, June 1, 2007; 97 (6): 4007-4016.

[\[Abstract\]](#) [\[Full Text\]](#) [\[PDF\]](#)

Fully Tuneable Stochastic Resonance in Cutaneous Receptors

J. B. Fallon and D. L. Morgan
J Neurophysiol, August 1, 2005; 94 (2): 928-933.

[\[Abstract\]](#) [\[Full Text\]](#) [\[PDF\]](#)

Stochastic Resonance in Muscle Receptors

J. B. Fallon, R. W. Carr and D. L. Morgan
J Neurophysiol, June 1, 2004; 91 (6): 2429-2436.

[\[Abstract\]](#) [\[Full Text\]](#) [\[PDF\]](#)

Stochastic Resonance within the Somatosensory System: Effects of Noise on Evoked Field Potentials Elicited by Tactile Stimuli

E. Manjarrez, G. Rojas-Piloni, I. Mendez and A. Flores
J. Neurosci., March 15, 2003; 23 (6): 1997-2001.

[\[Abstract\]](#) [\[Full Text\]](#) [\[PDF\]](#)

Medline items on this article's topics can be found at <http://highwire.stanford.edu/lists/artbytopic.dtl> on the following topics:

Neuroscience .. Computational Neuroscience
Veterinary Science .. Tibial Nerve
Physiology .. Nerves
Engineering .. Noise Levels
Statistics .. Correlation Coefficient
Physiology .. Rats

Updated information and services including high-resolution figures, can be found at:

<http://jn.physiology.org/cgi/content/full/79/4/1879>

Additional material and information about *Journal of Neurophysiology* can be found at:

<http://www.the-aps.org/publications/jn>

This information is current as of February 10, 2010 .

Noise-Induced Tuning Curve Changes in Mechanoreceptors

CHANDRA IVEY,^{1,2} A. VANIA APKARIAN,^{1,2} AND DANTE R. CHIALVO^{2,3}

¹Department of Neurosurgery and ²Computational Neuroscience Program, SUNY Health Sciences Center, Syracuse, New York 13210; and ³Division of Neural Systems, Memory and Aging, University of Arizona, Tucson, Arizona 85724

Ivey, Chandra, A. Vania Apkarian, and Dante R. Chialvo.

Noise-induced tuning curve changes in mechanoreceptors. *J. Neurophysiol.* 79: 1879–1890, 1998. Fibers from the tibial nerve of rat were isolated and spike activity recorded using monopolar hook electrodes. The receptive field (RF) of each recorded unit on the glabrous skin of the foot was mechanically stimulated with waveforms comprised of various frequency sine waves in addition to increasing levels of white noise. Single-unit responses were recorded for both rapidly adapting (RA) and slowly adapting (SA) units. Signal-to-noise ratio (SNR) of the output was quantified by the correlation coefficient (C_1) between the input sine wave and the nerve responses. The addition of noise enhanced signal transmission in both RA and SA fibers. With increasing noise, the initially inverted “V”-shaped, zero-noise tuning curves for RA fibers broadened and eventually inverted. There was a large expansion of the frequencies that the RA receptor responded to with increasing noise input. On the other hand, the typical shape of the SA fiber tuning curves remained invariant, at all noise levels tested. C_1 values continued to increase with larger noise input for higher frequencies, but did not do so at the lowest frequencies. For both RA and SA fibers the responses with added noise tended to be rate modulated at the low-frequency end, and followed nonlinear stochastic resonance (SR) properties at the higher frequencies. The changes in the tuning properties due to noise found here, as well as preliminary psychophysics data, imply that external noise is relevant for sensing small periodic signals in the environment. All current models of sensory perception assume that the tuning properties of receptors determined in the absence of noise are preserved during everyday tasks. Our results indicate that this is not true in a noisy environment.

INTRODUCTION

A tuning curve for a neuron is the measure of its responsiveness to changes in a given parameter. For example, measurement of individual neuron responses to stimuli at different frequencies and intensities results in frequency-response curves. The information processing capabilities of neurons in different sensory modalities, including vision, audition, and somatosensation, are based on the characteristics of these curves (Ikeda and Wright 1975; Leem et al. 1993b; Talbot et al. 1968). Experimentally determined frequency tuning curves have been considered invariant, implying a preferential response to environmental cues at best-tuned frequencies. This selective encoding based on tuning properties has been used to explain sensory perception (e.g., Bolanowski et al. 1988).

Researchers have focused on the differences in receptor responses to pure sine-wave frequencies (Johansson et al. 1982; Johnson 1974; Leem et al. 1993a,b; Mountcastle et al. 1972; Talbot et al. 1968). By compiling frequency-response information with other physiologically measured parameters

(conduction velocity and stimulus-response characteristics, for example), as well as by studying the anatomically different end organ structures of these neurons, general mechanoreceptor categories have been determined. For instance, slowly adapting (SA), rapidly adapting (RA), and Pacinian Corpuscles (PC) have been considered the main functional classifications for $A\beta$ mechanoreceptors.

Although frequency-response curves have been used to characterize mechanoreceptors physiologically (Johansson et al. 1982; Johnson 1974; Leem et al. 1993b; Talbot et al. 1968; Werner and Mountcastle 1965) and psychophysically (Bolanowski et al. 1988; LaMotte and Mountcastle 1975; Mountcastle et al. 1972), these studies have only looked at suprathreshold tuning, because by definition the measurement of tuning curves measures responses, and thus requires suprathreshold stimuli. When stimuli are subthreshold, or too weak to generate firing in the receptor, differential responses based on frequency are not definable, and tuning characteristics in this domain have not been available. This study is the first characterization of this unexplored domain of subthreshold frequency dependence of mechanoreceptors, i.e., subthreshold tuning curves, using weak stimuli in the presence of noise.

Recent developments have rediscovered that neuronal responses to weak subthreshold signals can be, at first sight, paradoxically enhanced by the addition of noise (Douglass et al. 1993). This enhancement is due to the cooperative effect of noise on signal because of the nonlinear properties of the neuron. This nonlinear enhancement of signal transmission by noise, related to the phenomenon of stochastic resonance (SR), has been studied in simulations of bistable systems (Bulsara et al. 1991; Wiesenfeld and Moss 1995), physical systems (Gammaitoni 1995; McNamara et al. 1988; Pantazelou et al. 1993), and biological systems: crayfish receptors (Douglass et al. 1993; Pei et al. 1996), rat mechanoreceptors (Collins et al. 1996), central sensory neurons, and psychophysical studies (Chialvo and Apkarian 1993; Simonotto et al. 1997). In these biological studies, the effects of noise have only been explored for fixed, or a narrow range, of sine-wave frequency stimuli.

Recently, a number of investigators have attempted to relax the definition of SR to include aperiodic phenomenon (Collins et al. 1995, 1996), broadband noise (Levin and Miller 1996), systems without dynamics (Wiesenfeld and Moss 1995), and systems without thresholds (Bezrukov and Vodyanoy 1997). To be precise, here we use the term SR in its earlier more restricted definition (Benzi et al. 1981; Fauve and Heslot 1983; Longtin et al. 1991), which applies to responses of a dynamical nonlinear system to weak periodic stimuli in the presence of noise. In such neuronal sys-

tems, the addition of noise increases the probability of firing on the average in “synchrony” with the period of the weak input. This probability increases with increasing noise to reach a maximum, and then, with even larger noise amplitudes, the relative probability of firing with the stimulus period decreases (Wiesenfeld and Moss 1995). The signature for this SR is “skipping” (i.e., the neuron fires or “skips” probabilistically only at the peak of the sinusoidal signal); giving rise to multi-peaked interspike interval histograms (ISIHS) (Longtin et al. 1991). Such ISIHS have been repeatedly published for RA and SA receptors during sinusoidal mechanical stimulation (see Talbot et al. 1968 for example), but these findings only recently have been related to noise-induced information transmission. For a superb review of the relevant body of results in between these fields, see Segundo et al. (1994).

This study examines changes in tuning properties of vibrotactile receptors with increasing noise levels and shows that, contrary to conventional intuition, the addition of noise to subthreshold periodic stimuli increases the bandwidth of the responses of RA and SA type fibers and eventually inverts the tuning curves of the RA mechanoreceptors. These changes may be related to the perceptual findings of the effects of noise on the discrimination of small input sine waves as studied here psychophysically. A conceptual model is proposed that predicts the observed noise-induced changes of the tuning curves.

This work was in partial fulfillment of the requirements for a Master’s degree in Neuroscience by the first author.

METHODS

Nerve preparation

Rats were initially anesthetized and maintained under 0.5% to 1.0% Halothane, 30% N₂O, and 60% O₂. Body temperature was maintained within normal ranges by a rectal thermometer connected to a feedback heating pad. The housing, care, and surgical procedures followed the institutional guidelines established by the Committee for the Humane Use of Animals. The back of the rat’s left foot was fixed to a dental cement casting to stabilize the preparation and to expose the footpad for mechanical stimulation. The left tibial nerve was isolated from the surrounding tissue, and the proximal side of the nerve bundle was severed and placed on a dissecting plate. A well was made with skin flaps and filled with mineral oil. The perineural sheath was opened by microdissection, and small bundles of fibers were teased from the nerve and placed on a silver monopolar hook electrode. The reference electrode was placed in nearby muscle. Receptive fields (RFs) on the footpad were tested with small glass probes until single-unit activity could be found. Fibers chosen had fields confined to the glabrous skin of the footpad and responded to touch.

Stimulation and recording

Once a responsive unit was identified, a mechanical stimulator was set up over the RF. The equipment used for mechanical stimulation has been described (see Werner and Mountcastle 1965). Briefly, a magnetically driven stylet is servo-controlled to follow input displacements. The stimulator was attached to a computer that generated both sine wave and noise (uniformly distributed), using a D/A card. The computer output was additionally low-pass filtered with a 2-kHz cutoff. Fourier analysis of the noise as measured from the output of the stimulator indicated a Lorentzian

distribution with energies spread to ~500 Hz. Thus the noise can be considered essentially white in the range of frequencies of interest (0–80 Hz). A rounded (~1 mm wide), plastic tip was used to stimulate the RF. The tip was positioned at the most sensitive location of the RF such that it touched the skin without producing any firing.

Isolated single-fiber responses were amplified, displayed, and collected by a computer acquisition system (Datawave Technologies). Zero noise tuning curves were determined by stimulating the fibers with 20 cycles of different frequency sine waves (0.1–70 Hz) at constant displacement amplitudes. The amplitude of stimulation was decreased until distinct frequency dependence in the fiber’s response could be recorded. This information was used to categorize the units as RA or SA, because RA units have greater responses to higher frequencies and SA units respond better to increasingly lower frequencies. At least 10 series of 10-s stimuli for each value of sine-wave amplitude and incrementing noise variances between 0 and 1,600 μ m (5–10 increments) were then generated, and the fiber’s responses were recorded. Data were analyzed off-line to characterize changes in the unit response to frequency and increasing noise levels.

Data analysis

After acquisition, all data were clustered based on peak time and spike amplitude using a factor-analysis clustering program (Datawave Technologies) to ensure the isolation of single-unit responses. From these analyses, interspike intervals were obtained, which were used for studying response properties.

ISIHS were created to examine phase-locking and skipping behavior. Period histograms were created by dividing each period into 20 bins and measuring the mean count over the total number of cycles. These binned data were also used to calculate the correlation coefficient. The linear correlation coefficient, or C_1 , was calculated as

$$\langle C_1 \rangle = \frac{\overline{S(t)[R(t) - \overline{R(t)}]}}{[\overline{S^2(t)}]^{1/2} \{[\overline{R(t) - R(t)}]^2\}^{1/2}}$$

where $S(t)$ is the zero mean input signal, $R(t)$ the period histogram, $\langle \rangle$ signifies ensemble estimate, and overbars are averages.

Definitions for threshold

The definition of a weak signal is necessarily operational. The value of the threshold of a neuron is time dependent. Thus a signal is defined as “subthreshold” only for a given frequency because a given amplitude sine wave could produce no response at one frequency, yet induce spikes at another. For this reason ad hoc criteria need to be used. For RA units, threshold was defined at the most sensitive frequency as the stimulus giving rise to 0.5 spikes per sine-wave cycle. Various increments of sine-wave amplitudes around this threshold amplitude were tested. In the case of the SA-classified fibers that respond better to increasingly low frequencies, threshold was defined as a sine-wave amplitude giving rise, on average, to 0.5 spikes per cycle at the highest frequency tested.

Psychophysics

Subjects rested one finger on a mechanical stimulator with a 1-mm, rounded plastic tip (the same stimulator as above). They were tested with a two-alternative-forced-choice paradigm (Watson and Pelli 1983) during which they were asked to attend to the fingertip stimulation and to discriminate which of two time epochs contained a sine-wave stimulus in the presence of noise. One time epoch contained a given level of noise alone, whereas the other contained the same level of noise added to a small sine wave of a given

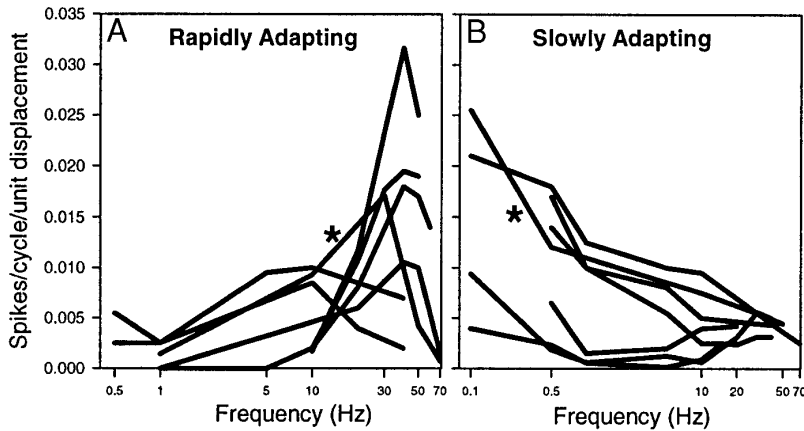


FIG. 1. Tuning curves for 14 units recorded during this study. *A*: rapidly adapting (RA) units. *B*: slowly adapting (SA) units. Average responses to 20 cycles at given frequencies were recorded and divided by amplitude of input. RA and SA units were categorized based on their relative responses to high- vs. low-frequency stimulation. Those firing more in response to high-frequency were listed as RA, whereas those having a greater response to low frequency, or a region where response decreased with increasing frequency, were categorized as SA. Tuning curves of the RA and SA fibers analyzed in Figs. 3–6 are marked here with asterisks.

frequency (3 or 30 Hz). The amplitude of the sine wave was adjusted during successive trials. Threshold was defined for a specific sine wave-plus-noise test stimulus as 75% correct. Each test stimulus (sine wave-plus-noise level) was tested a minimum of two times, and a maximum of six times. The thresholds for different sine wave-plus-noise trials were then plotted versus the noise level used.

RESULTS

Seven RA units and seven SA units (see Fig. 1) were studied in a total of seven animals. Although various ranges of input frequencies, at different sine-wave amplitudes and with the addition of multiple noise levels, were used to test individual fibers, consistent changes in the tuning curves were seen for each category of fibers. For better presentation of the emergent commonalities, here we present results mainly from one RA and one SA for which the most extensive range of testing was accomplished (tuning curves marked with asterisks in Fig. 1, *A* and *B*, respectively). These experiments display many changes in the responses of the SA- and RA-categorized fibers for which there was no previous theoretical interpretation. The major trends discovered are presented here and later discussed in the light of formal arguments from the theory of noise-perturbed nonlinear systems.

Nonlinear amplification of signal transmission

Figure 2 illustrates the nonlinear enhancement of a weak signal transmission by the addition of noise. This nonadditive quality is shown in a RA unit stimulated with an input frequency of 1 Hz. Figure 2*A* displays the period histogram of the unit response to sine-wave stimulation at 210- μm peak-to-peak skin displacement without external noise. This amplitude sine wave is subthreshold at this frequency, thus no firing is recorded. The second panel (Fig. 2*B*) displays the period histogram when only noise with a variance of 620 μm is used to stimulate the same unit. The response to this noise input shows a relatively uniform firing throughout the duration of the stimulus, which results in a flat period histogram. When these two mechanical stimuli are added and presented together (Fig. 2*C*), there is a marked increase in firing in-phase with the sinusoidal input that cannot be accounted for by the responses to each presented alone. The information transmission in this fiber during sine-wave input

alone is zero, i.e., the correlation coefficient $C_1 = 0.00$. When noise alone is presented $C_1 = 0.04$, and when both stimuli are presented together $C_1 = 0.78$. The latter is a measure of the extent of nonlinear amplification of information transmission with the addition of noise.

Period histograms

Period histograms can demonstrate many of the properties of the unit responses when the input is modulated by noise. Figure 3 shows example period histograms for a RA and a SA type fiber. Figure 3*A* shows periodic histograms for a RA unit stimulated at five different frequencies (1, 10, 30, 50, and 70 Hz) at a constant sine-wave amplitude (40 μm), with noise variance increasing from 0 to 1,560 μm . The first row of the figure shows the responses to the sine wave with no noise. These responses approximate the zero-noise tuning curve of the fiber. Responses are close to threshold for 30 and 50 Hz (0.4 and 0.32 spikes per cycle, respectively), and

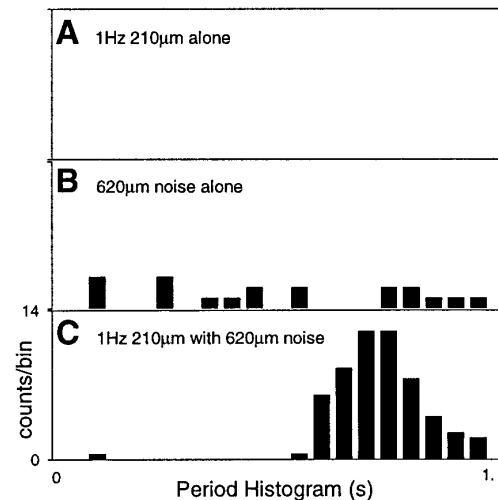


FIG. 2. Period histograms of RA unit's responses to stimulation by subthreshold 1-Hz sine wave at 210 μm (*A*), white noise at 620 μm (*B*), and sine wave as in *A* plus white noise as in *B* (*C*). The response of the unit markedly increases firing in phase with the sinusoidal input when both the subthreshold sine wave and the noise are presented together. All data are binned into 20 bins and then total counts recorded to create period histograms. Each part of this figure created from one data set for the unit. The y-axis scales are linear and the same for *A*–*C* panels, and correspond to that shown in *C*.

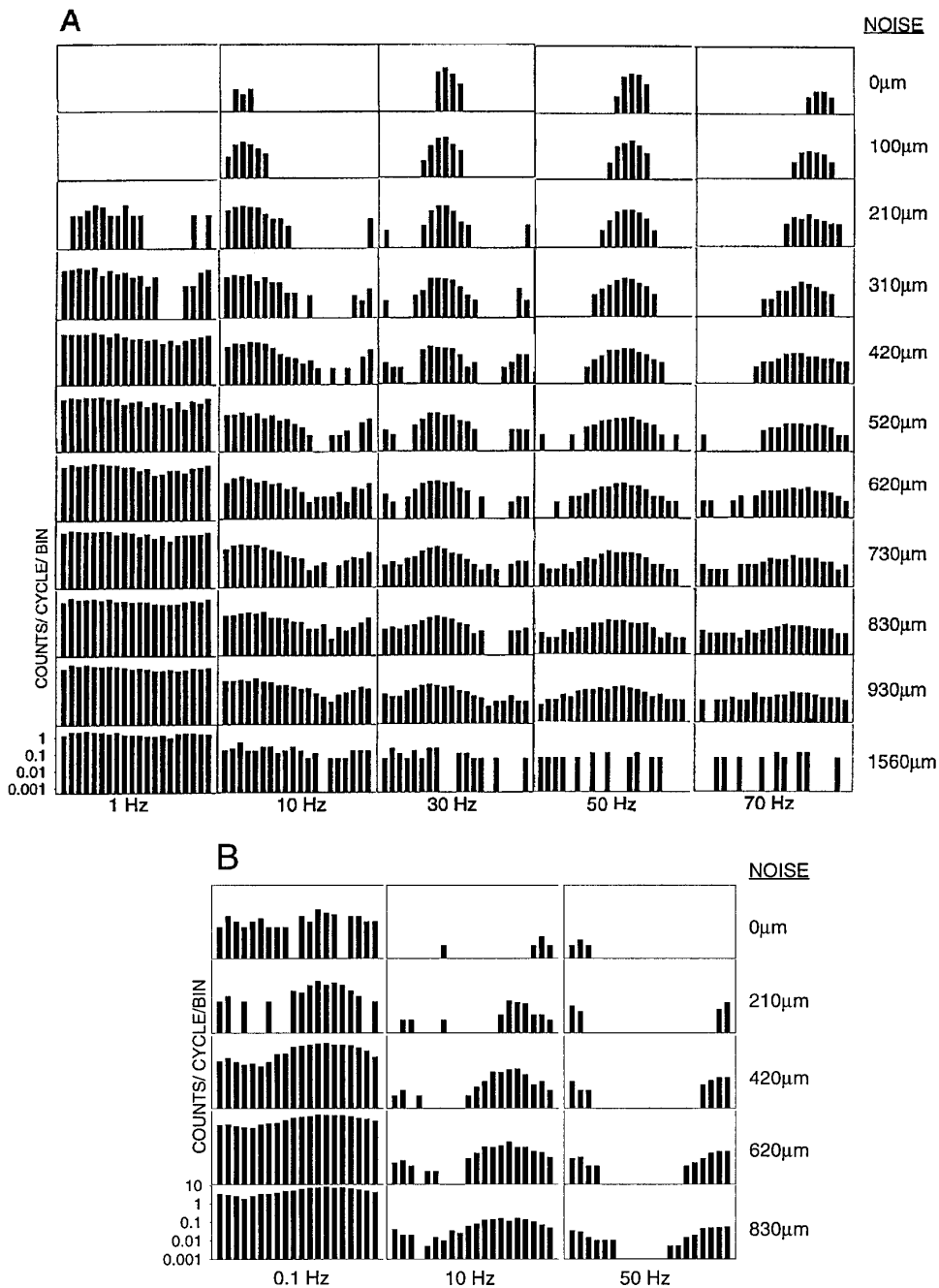


FIG. 3. Period histograms for a SA and a RA fiber (tuning curves identified by asterisks in Fig. 1). *A*: series of histograms for RA unit with 40- μm amplitude input sine waves of 1, 10, 30, 50, and 70 Hz with added noise amplitudes of 0, 100, 210, 310, 420, 520, 620, 730, 830, 930, and 1,560 μm . *B*: series of histograms for SA unit with 50- μm amplitude input sine waves of 0.1, 10, and 50 Hz with added noise amplitudes of 0, 210, 420, 620, and 830 μm . All data are binned into 20 bins and average counts/cycle/bin are plotted with the same log scale, as shown for *bottom left panel*. The time duration plotted for each frequency column corresponds to a single period, i.e., the 1-Hz column time scale is 0–1.0 s, for the 10-Hz column time scale is 0–0.1 s, and so on. Each part of this figure created from the average of 2 complete data sets for each unit.

are below threshold at 1, 10, and 70 Hz. Within any column (a given frequency), descending graphs indicate increased firing rate with increasing levels of noise. Although the mean firing rate per cycle (the area under the period histograms) is highest at the most sensitive frequencies for low noise levels (0–210 μm), at higher levels the firing rate monotonically decreases with increasing frequency. Generally, responses are more rectified, or nonlinear, for higher frequencies. However, the transition from rectified responses to rate-modulated, or linear, responses are observed for different noise levels at each frequency. This transition requires the largest amount of noise around the most sensitive frequency (determined by the zero-noise tuning curve). At the largest noise levels (1,560 μm amplitude) the linear responses are

destroyed as well, and the unit's firing is only a function of the noise amplitude. The responses of this RA unit are phase shifted with the sine-wave frequency, but increasing noise does not modulate the phase shift.

Period histograms for one SA unit at three frequencies (0.1, 10, and 50 Hz, input amplitude of 80 μm) and five different noise variances (0–830 μm) are shown in Fig. 3*B*. Zero-noise histograms (noise = 0 μm , *top row*) show mean firing of 2.7 spikes/cycle at 0.1 Hz, but only 0.03 and 0.02 spikes/cycle at 10 and 50 Hz, respectively. With increasing noise (210, 420, 620, and 830 μm), the histograms better approximate the period of the sinusoid at all frequencies tested. The histograms also show that the response patterns of the neuron at the high-frequency (50 Hz) are rectified,

and those at the midrange frequency (10 Hz) are somewhat rectified at low noise levels but become linear with greater increases in noise. The lowest frequency (0.1 Hz) responses are not rectified. The transition from rectified to rate-modulated responses occurs with the largest amount of input noise for 10 Hz, but does not occur at 50 Hz with the noise variances tested. Higher noise levels would result in linear responses at the high-frequency ranges (seen in other SA fibers). The mean response per cycle for the SA decreased monotonically with increasing frequency at all noise levels.

Overall, the SA period histogram patterns are similar to the patterns shown in the first three columns of the RA period histograms at intermediate levels of noise. The addition of noise to the low-frequency stimuli in the RA unit parallel the SA responses to sine waves in noise, whereas the high-frequency noise dependence in the RA is unique to this type of fiber.

ISIHs

The ISIHs indicate response properties that in many ways complement the patterns seen in period histograms. Figure 4 displays the corresponding ISIHs for the same RA and SA unit as shown in Fig. 3. The ISIHs for mid to high frequencies in the RA (10–70 Hz in Fig. 4A) with low levels of noise (0–420 μm) show multi-peaked distributions with the first peak occurring at the sine-wave period, and the later peaks occurring at multiples of the applied period. The peak heights decay linearly in these log-linear ISIH plots. As noise is increased, the distributions shift toward the first peak, indicating that the unit responds with less skipping between cycles. Together, these properties of ISIHs are termed noise-induced phase locking or stochastic resonance and are preserved for higher noise levels (up to 730 μm) around the most sensitive frequency (30 and 50 Hz, determined at zero-noise). At the extreme frequencies (1, 10, and 70 Hz) and especially at high noise amplitudes (>520 μm), the ISIHs have unimodal distributions. The unimodal distributions are different at low (e.g., 1 Hz) and high frequencies (e.g., 70 Hz). The low-frequency distributions are limited to intervals much smaller than the stimulus period indicating rate-modulated responses. The high-frequency distributions are spread through time intervals covering a range up to seven times the multiple of the stimulus period. The latter effect is due to noise introducing jitter on the multi-peaked responses.

The SA unit's ISIHs for three sine-wave frequencies and five noise levels are displayed in Fig. 4B. These ISIHs of the RA and SA units show a correspondence similar to that observed between their period histograms in Fig. 3. The ISIH patterns for the SA are similar to the patterns shown in the *first three columns* of the RA ISIHs at intermediate levels of noise.

Correlation coefficients (C_1) for RA unit

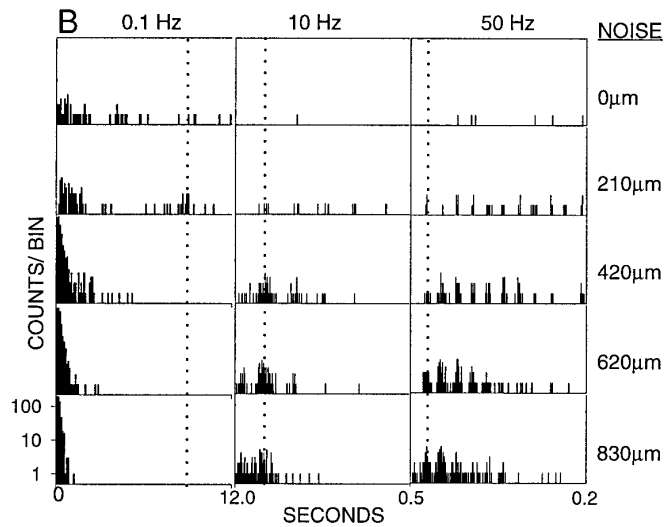
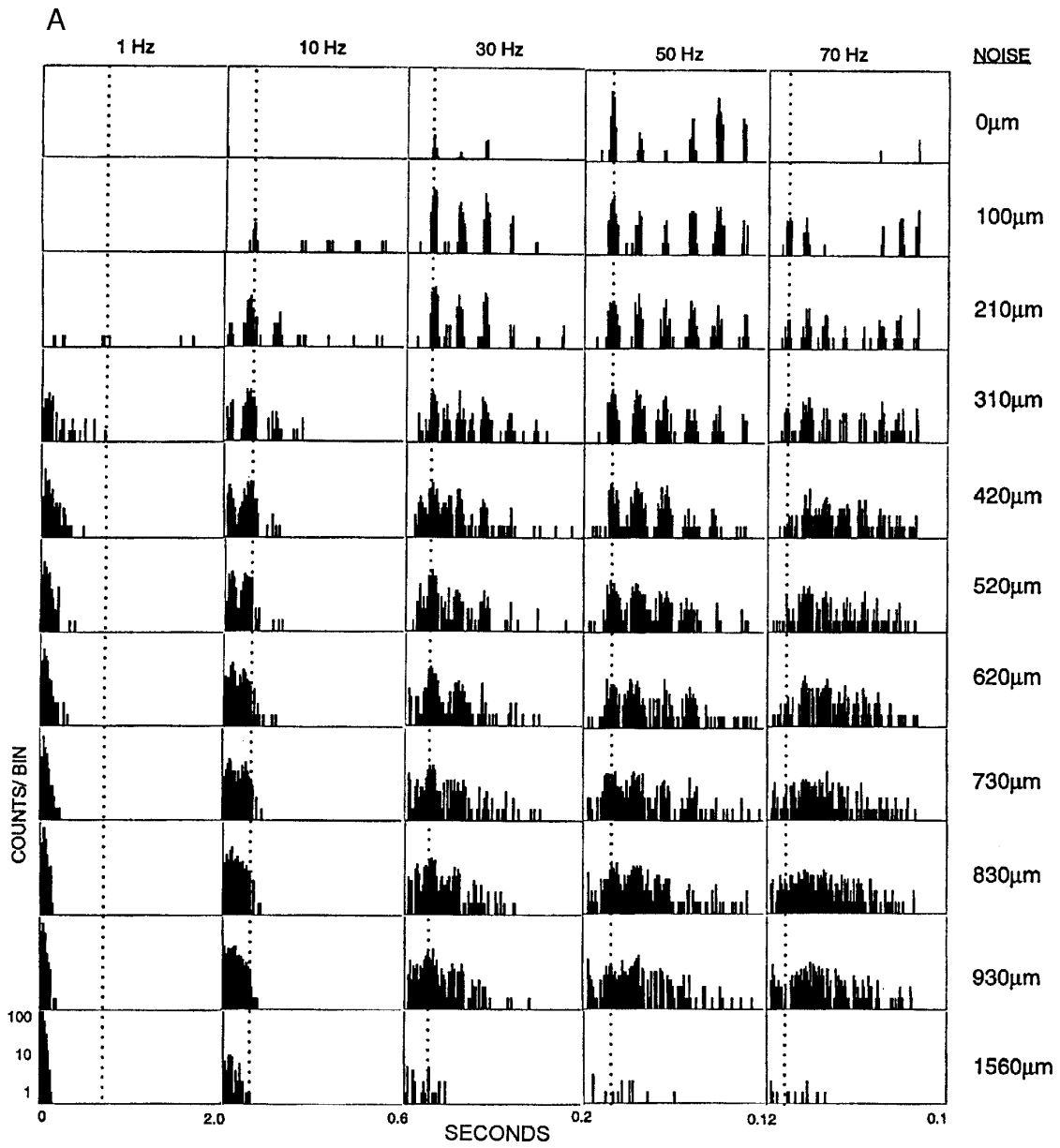
Period histograms and ISIHs display in a quantitative way the linear and nonlinear responses of SA and RA fiber responses to modulation by noise. C_1 quantifies the linear response of signal transmission, and with certain caveats (Chialvo et al. 1996; Collins et al. 1996) the signal-to-noise ratio (SNR). Therefore we use C_1 to determine changes in the

tuning curves with added input noise. Figure 5 shows SNR measured by C_1 for the RA fiber shown in Figs. 3 and 4. This unit was tested over five frequencies and three input sine-wave amplitudes (20, 40, and 80 μm for A, B, and C, respectively). These three sine amplitudes correspond to just below, at, and above threshold stimuli for the zero-noise responses (Fig. 5B shows C_1 values for the same data presented in Figs. 3A and 4A). Although many noise levels were tested, six representative levels are shown in Fig. 5, A–C, where changes in frequency tuning are illustrated as a function of noise.

The zero-noise curve at the lowest input sine amplitude (20 μm , Fig. 5A) approximates the tuning curve of this unit (starred RA tuning curve in Fig. 1). No responses occur for the lowest frequency (1 Hz) stimuli without noise; thus C_1 values here are zero. C_1 for this frequency peaks at a value of 0.55 (at 520- μm noise) and does not change with larger increases in input noise. Zero-noise responses for both 10 and 70 Hz also show no responses at this input sine-wave amplitude and thus have C_1 values of zero. The C_1 values increase to 0.8 for both (at 520- μm input noise for 10 Hz, and at 210- μm noise for 70 Hz), and then, with even higher noise input, both decrease to 0.35. C_1 values for 30 and 50 Hz at 20- μm input sine amplitude are similar to one another. At zero noise they already exhibit C_1 values >0.5. These values increase with added noise to 0.9 and 0.8 for 30 and 50 Hz (both with 520- μm input noise), respectively, and then decrease substantially to <0.5 at the highest noise level (C_1 values of 0.4 and 0.1 for 30 and 50 Hz, respectively).

Each curve in Fig. 5A indicates the tuning curve of the fiber at a different noise level. The zero-noise tuning curve shows sensitivity of this RA to middle frequency sine waves (30 and 50 Hz). With the addition of noise, the tuning curves show increasing C_1 values at all frequencies, thus broadening the responsiveness to include the whole range of frequencies tested. The highest amplitude noise tested (1,560 μm) shows an inverted tuning curve from that at zero noise, i.e., the C_1 values for low (1, 10 Hz) and high frequencies (70 Hz) are larger than those of the zero noise curve, but C_1 values around the middle frequencies (30 and 50 Hz) have decreased below their initial values.

At higher amplitude sine-wave inputs, the C_1 values for RA responses show some differences when compared with the responses described for the lowest sine-wave amplitude tested. The zero noise C_1 values for these 40- and 80- μm sine waves (Fig. 5, B and C, respectively) do not mirror the tuning curve of the unit because responses are now present for stimulation at 10 and 70 Hz as well. No responses, and thus a C_1 value of zero, are only exhibited at 1 Hz. At 1 Hz, there is a much larger increase in C_1 with increasing noise amplitude than seen previously at this frequency, and the C_1 values peak at 0.8 (520- μm noise) with 40- μm sine amplitude and 0.95 (1,560- μm noise) with 80- μm sine amplitude. With each of the other frequencies, there are increases in C_1 values (between 0.4 to 0.9 with up to 934- μm noise), but then C_1 markedly decreases for most frequencies at the highest noise level (1,560 μm). At these two larger input amplitudes, higher frequencies (30–70 Hz) consistently showed a larger decrease in C_1 at the highest noise levels, whereas the lowest frequency (1 Hz) never showed a decrease in the noise range tested. These amplitudes of sine input also



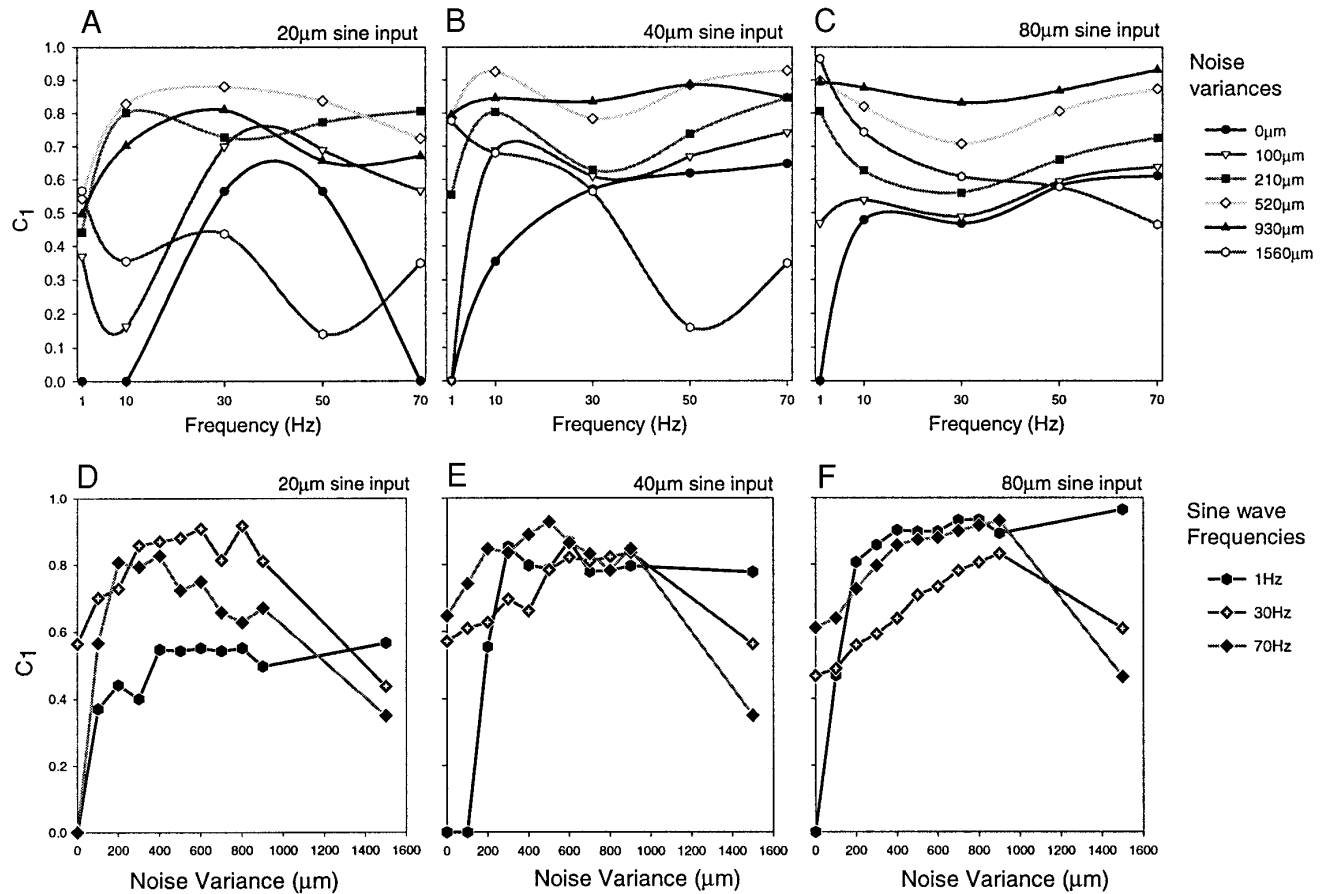


FIG. 5. Changes in tuning curves for RA unit, measured quantitatively by C_1 . These data are from the same RA fiber displayed in Figs. 3 and 4. *A–C*: frequency dependence of C_1 for 6 input noise levels, 5 input sine-wave frequencies, studied for 3 sine amplitudes. *D–F*: replot the same data as in *A–C* as a function of noise amplitude for 3 frequencies. *A*: C_1 values for input sine amplitude of 20 μm and input noise amplitudes of 0, 100, 210, 520, 930, and 1,560 μm . Midrange noise inputs (100–930 μm) show a broadening of the tuning curves at zero noise. The highest noise level, 1,560 μm , shows an inversion of the zero-noise tuning curve. C_1 values for input sine amplitude of 40 μm (*B*) and 80 μm (*C*) are also plotted for responses with input noise amplitudes of 0, 100, 210, 520, 930, and 1,560 μm . *D*: C_1 values for input sine amplitude of 20 μm , 3 frequencies, and 11 input noise amplitudes. *E* and *F*: the C_1 values when the sine-wave amplitudes are increased to 40 and 80 μm , respectively. The standard error of the mean C_1 ranged between 0.2 and 0.5.

displayed inverted tuning curves at the highest noise in comparison with the zero-noise tuning curves. A similar inversion of the tuning curves were seen in four of the seven RA units examined. In two cases where the inversion was not observed, the maximum noise levels used was less than those in the rest.

Overall, there seems to be a systematic change in noise modulation of tuning curves across the three sine amplitudes. With increased sine amplitudes, C_1 values at zero-noise input increase. Also, with these increased sine

amplitudes, and at the highest noise levels, the inverted tuning curves become broader.

Figure 5, *D–F*, presents portions of the same data as in Fig. 5, *A–C*, to clarify the dependence of C_1 on input noise amplitude. Responses to 3 sine-wave frequencies (1, 30, and 70 Hz) and 11 noise increments (0–1,500 μm) are shown. For the sine input at subthreshold amplitude (20 μm), C_1 values are highest for the 30-Hz sine wave, over most intermediate noise levels (Fig. 5*D*). When the sine-wave amplitude is increased to be closer to threshold (40 μm), C_1 becomes more similar across all three frequencies (Fig. 5*E*)

FIG. 4. Interspike interval histograms (ISIHS) for same SA and RA fibers shown in Fig. 3. *A*: RA plots from stimulation with 1, 10, 30, 50, and 70 Hz sine wave of 40- μm amplitude with increasing noise input from 0 to 1,560 μm . *B*: SA plots from stimulation with 0.1, 10, and 50 Hz sine wave of 50- μm amplitude adding noise input from 0 to 830 μm . ISIHS can show many of the linear and nonlinear regions of unit responses as they are modulated by noise. Dotted lines denote the stimulation period. Bin sizes for *A* are 0.02, 0.06, 0.002, 0.0012, and 0.001 s for 1, 10, 30, 50, and 70 Hz, respectively. Stimulation of each frequency with 1,560 noise used only 20 input cycles instead of the larger number of cycles used at lower noise amplitudes. Analysis of the 1st 20 cycles of the lower noise data sets gives the same general results as the analysis of the whole data set, thus the results for these 20 cycles are also considered to show consistent results. Bin sizes for *B* are 0.008, 0.001, and 0.0005 s for 0.1, 10, and 50 Hz, respectively. Each part of this figure plotted for 1 data set for each unit. Counts/bin are plotted in log scale as shown in *bottom left panel*.

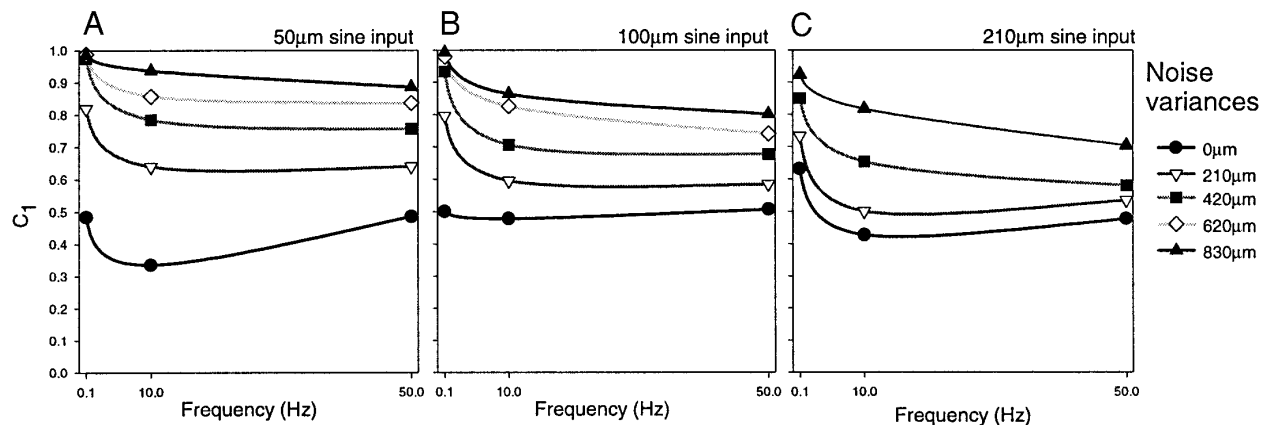


FIG. 6. Changes in tuning curves for SA unit as measured quantitatively by C_1 . These data are from the same SA fiber displayed in Figs. 3 and 4. A: C_1 values for input sine amplitude of $50 \mu\text{m}$ and input noise amplitudes of 0, 210, 420, 620, and $830 \mu\text{m}$. Midrange and large noise input (210– $830 \mu\text{m}$) show similar increases in C_1 at all frequencies. C_1 values for input sine amplitude of $100 \mu\text{m}$ (B) and $208 \mu\text{m}$ (C), both with input noise amplitudes of 0, 210, 420, and $830 \mu\text{m}$, show shifts in C_1 that parallel those seen at sine input of $50 \mu\text{m}$. Each part of this figure created from the average of 2 complete data sets for the unit.

for most intermediate noise levels. Further increasing the sine-wave amplitude ($80 \mu\text{m}$, above threshold) reverses the frequency dependence of the relationship between C_1 and noise (Fig. 5F). In this case the 30-Hz sine-wave input results in the lowest C_1 values for most noise levels, as compared with the 1- and 70-Hz C_1 values as a function of input noise amplitude. The 30- and 50-Hz responses are not shown in Fig. 5, D–F, for clarity. However, their C_1 values follow the same pattern as shown. The C_1 values for these two frequencies are intermediate between the 30-Hz and the 1- and 70-Hz responses, at low- and high-input sine-wave amplitudes and are at about the same values as the other three frequencies for the intermediate input sine amplitude. Thus the peak C_1 across the noise levels examined (which is different for different frequency sine-wave inputs) also undergoes an inversion. In this case, however, the inversion is a function of the sine-wave amplitude.

Correlation coefficients (C_1) for SA unit

Changes in SA fiber tuning curves with the addition of noise were also quantified using C_1 , as shown in Fig. 6. This unit was tested over three frequencies and three input sine-wave amplitudes (50, 100, and $210 \mu\text{m}$ for A, B, and C, respectively). Figure 6A shows the C_1 values that correspond to the data in Figs. 3B and 4B.

Zero noise trials for the lowest sine amplitude ($50 \mu\text{m}$, Fig. 6A) show that the C_1 value is highest at 0.1 Hz, decreases at 10 Hz, and then increases again at 50 Hz. The tuning curve shows similar C_1 values with both 100- and 200- μm sine-wave amplitude (0- μm noise, Fig. 6, B and C). With the addition of noise, C_1 values at 0.1 Hz rapidly approach 1.0 at all sine amplitudes. Values at 10 and 50 Hz also increase with added noise, but as sine-wave amplitude is also increased, the maximum C_1 value decreases (0.9 for $50 \mu\text{m}$, 0.8 for $100 \mu\text{m}$, and even lower for $200 \mu\text{m}$ sine amplitude). Increasing sine amplitude does not substantially change the low-frequency range of unit's tuning curve or its modulation by noise, but decreases the high-frequency range. Addition of greater input noise values increases C_1

values in all cases shown without affecting the shape of the tuning curve. The noise levels tested were not high enough to reach a region where decreases in C_1 would occur. All other SA units were examined in the same noise range and none (7 of 7) showed C_1 decreases at high noise levels.

Psychophysics

Data sets from three subjects are shown in Fig. 7. Figure 7A shows sine-wave thresholds for stimulations of 3 Hz with increasing noise amplitude, and Fig. 7B shows sine-wave thresholds for 30 Hz with increasing noise. The threshold amplitudes for 3 Hz were higher than those for 30 Hz, but the shape of the curves are consistent within each frequency, regardless of subject. Also, the standard deviations recorded for trials at 3 Hz were larger than those recorded for 30 Hz, but the magnitude of these standard deviations were consistent between subjects. This trend for consistently large standard deviations has been found elsewhere (Makous et al. 1995).

As shown in Fig. 7A, there is a region for stimulation with 3 Hz in which sine-wave thresholds are lower within a nonzero region of noise. The thresholds then increase as the noise amplitude becomes larger. This same trend is not obvious for sine-wave stimulations of 30 Hz (Fig. 7B).

DISCUSSION

The results presented are derived from fibers where a large range of input noise levels and sine-wave amplitudes and frequencies were tested. However, the features presented apply mainly to the specific regions explored. The RA fibers studied in early experiments were examined for a smaller range of input noise (up to 500–600 μm) and for sine-wave amplitudes that were either high above threshold or far below threshold. The experiments that resulted in more informative data were those where the sine-wave amplitudes were just around threshold and covered the largest range of noise (5 units). The ranges of frequencies studied, as well as the noise ranges used, were limited by the mechanical properties

of the stimulator. In many cases, we could not examine the high-frequency range of the RA fibers (>70 Hz). The range of noise amplitudes used to study RA fibers was from 0 to $1,560 \mu\text{m}$, whereas for SA the maximum range covered was $0\text{--}900 \mu\text{m}$. Therefore noise modulation of the highest frequency portion of the tuning curves for RA fibers and for highest noise amplitudes for the SA fibers remain to be explored.

Correlation coefficient, C_1 , was used as a quantitative measure of SNR. This is a linear measure, but, as pointed out in the results (for further discussion see Chialvo et al. 1996), the responses of the fibers have linear and nonlinear ranges. The addition of noise effectively creates a smoother transition from the sub- to suprathreshold regime in any system with a sharp threshold (e.g., a neuron). Because the latter is a linearizing effect, C_1 can be used, but does not describe other nonlinear effects (see Chialvo et al. 1996; Segundo et al. 1994).

The primary findings of this study are as follows. 1) The addition of noise enhances signal transmission in both the RA and SA fibers. 2) With increasing noise, the zero-noise tuning curves for RA fibers are broadened and are eventually inverted. There is a large expansion of the frequencies that the RA receptor responds to with increasing noise input. Increases in input sine amplitude shift the tuning curves in a systematic complicated pattern. These changes in RA tuning curves with noise in the low-frequency range can be interpreted as a conversion of the RA-type fiber responses into SA-type responses. Such noise-modulated changes in RA type

receptors have been described in the past for crayfish stretch receptors (Buño et al. 1978), and for the elasmobranch utricle (Macadar et al. 1975). 3) With increasing noise, the shape of the SA fiber tuning curves remains invariant. C_1 values continue to increase with larger noise input for higher frequencies; at the lowest frequencies, C_1 reaches a maximum with relatively small amounts of noise and does not change further. Increases in input sine amplitude do not affect the low-frequency range of the tuning curves, but decrease the high-frequency end. 4) Responses for both RA and SA fibers with added noise tend to be rate modulated at the low-frequency end and follow SR properties at the higher frequencies. 5) The preliminary psychophysical results suggest noise enhancement of touch perception at least for the lower frequency tested.

These results show that touch receptors exhibit properties of stochastic resonance (i.e., regions where the ISIH denote skipping), over a large range of input noise amplitudes, regardless of receptor classification (as SA or RA). The responses of these fibers show parameter regions of linearization by noise, as well; low-frequency and high noise responses show rate coding in both period histograms and ISIHs for both RA and SA fibers. Also, RA fibers show linear responses at very high frequencies with large amounts of input noise. Although there is a growing body of work regarding the linear and nonlinear effects of noise on signal transmission, there is no general theory to explain modulation of tuning curves as a function of input noise and signal amplitudes. The theory of SR explains changes in period histograms and ISIHs for a given stimulus amplitude and frequency (some of the columns in Figs. 3 and 4). However, SR theory has been developed in model neurons and studied in biological system without considering interactions of noise with tuning. Noise-induced linearization of the neuron transfer function was recently explored by Chialvo et al. (1996), where the transition from nonlinear to linear responses to noise as a function of stimulus frequency was investigated on a FitzHugh-Nagumo model neuron. The period histograms generated for this model neuron (Fig. 11, Chialvo et al. 1996) closely correspond to the low frequency and high noise portions of our results. The model does not describe the linear responses seen at the highest frequencies and large noise input in the RA and does not explore the stimulus amplitude dependence of noise modulation. Simulations that use a "tuned" model neuron corresponding to the dynamical properties of touch receptors are needed to better understand the noise modulation of RA and SA tuning curves.

Collins et al. (1997) recently reported enhancement of human tactile perception by noise. Although our psychophysical studies are preliminary, they do suggest touch perception enhancement with noise at least at 3 Hz. Moreover, the data show that the noise effects for touch perception are frequency dependent because the perception enhancement with noise for the 3-Hz stimulus is observed in a range where the 30-Hz stimulus shows minimal, if any, noise enhancement. The latter difference is consistent with the differences in noise enhancement of signal transmission we observe between RAs and SAs. The noise amplitudes used for these experiments were all above threshold, i.e., the subjects could clearly feel the presence of noise. It is possible that sub-

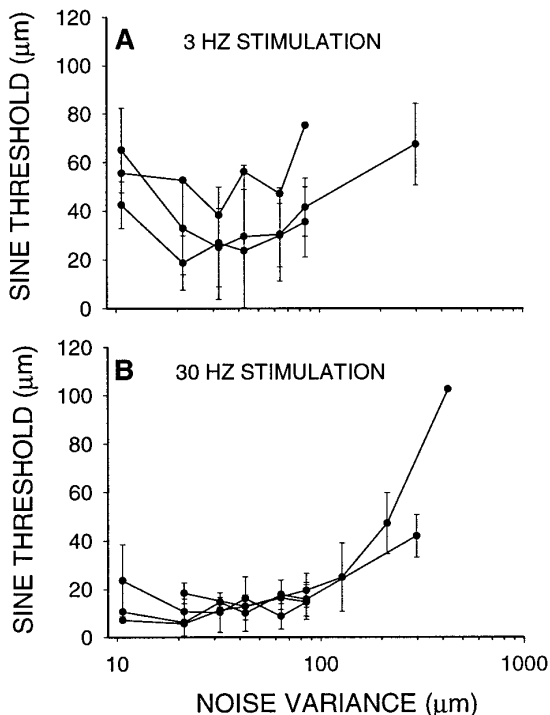


FIG. 7. Preliminary psychophysics results for 3 human subjects. *A*: thresholds for stimulation with 3-Hz sine wave with the addition of noise. These results demonstrate a nonzero noise region in which thresholds for discrimination of the sine wave are lower. *B*: thresholds for stimulation with 30-Hz sine wave with the addition of noise. Each point is the average of 3–6 individual trials. The standard deviations are for each subject calculated for repeated tests.

threshold noise amplitudes may be more effective for enhancing touch perception at the high frequency, but remains to be tested.

Model for noise modulation of tuning curves

The main features of the results can be captured using the conceptual model shown in Fig. 8. This figure consists of three diagrams; A shows the expected SNR, measured by C_1 , for a tuned model neuron stimulated at three input frequencies (distinguished as low, medium, and high). The curves are expected assuming the properties of non-linear excitable systems seen in previous work (Chialvo

et al. 1996; Collins et al. 1996). The only difference here is that in the *middle panel* the curve is shifted according to the distance to threshold as shown in Fig. 8B. The distance to threshold is different either because the signal is attenuated (as shown in B), or the threshold itself moves with different frequency inputs. Figure 8B shows the intracellular membrane potential variation with respect to the neuron's threshold expected for the three frequencies considering the mechanoelectric transfer function of a RA receptor (e.g., see Bell et al. 1994). Figure 8C shows the ensuing tuning curves for the low-noise, medium-noise, and high-noise situations, where the relative magnitude at each frequency is reflected by the empirically de-

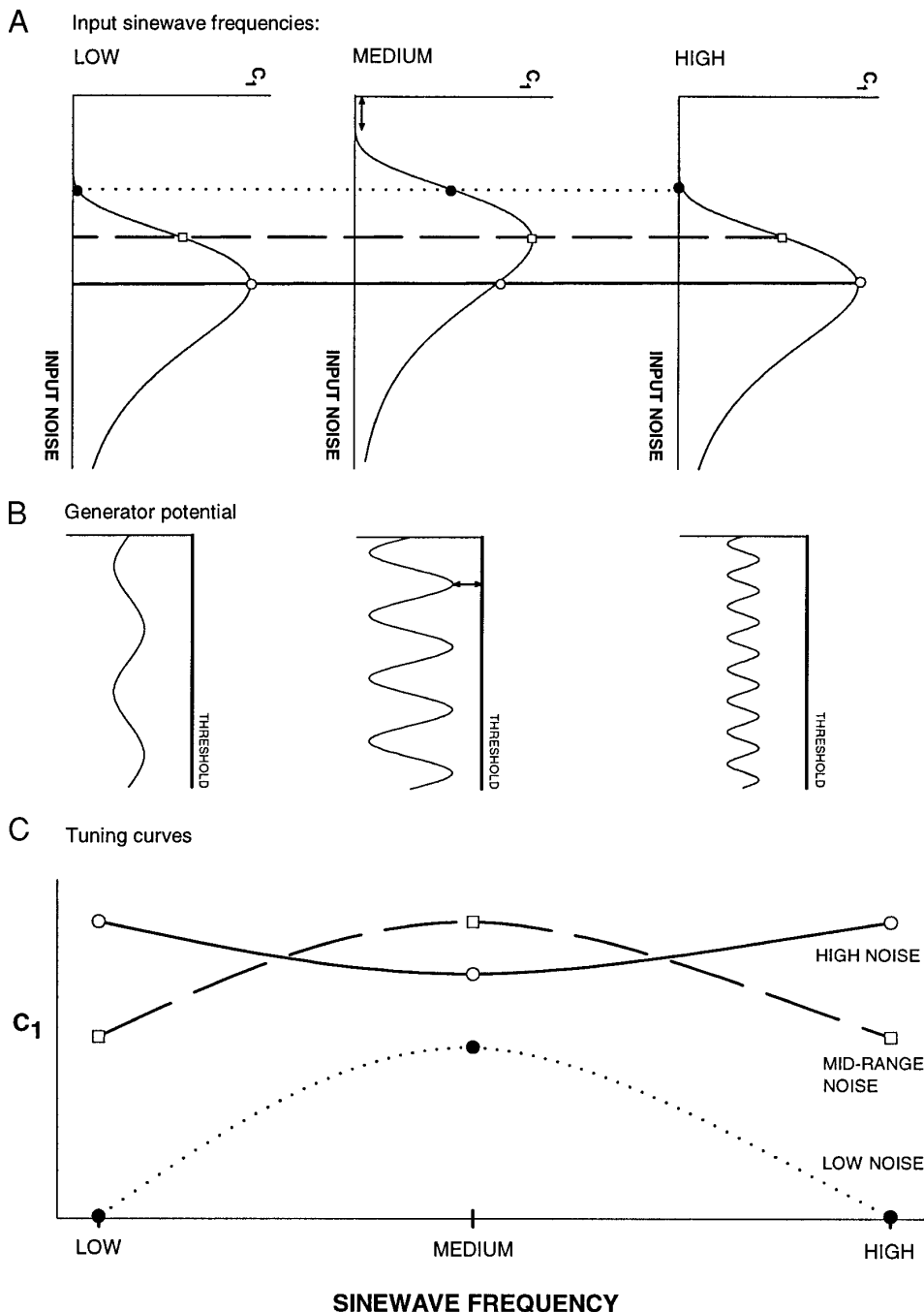


FIG. 8. Conceptual model for tuning changes due to noise in neural receptors. The frequency dependence of the receptor is assumed to determine the amplitude of the generator potential relative to threshold. The figure illustrates the model by plotting the receptor response to 3 frequencies. Each component has its own peculiar noise dependence of signal-to-noise ratio (SNR), as measured by C_1 . A: dependence of C_1 on input noise for 3 input sine-wave frequencies: low, medium, and high. The various shapes of the 3 C_1 -noise curves may be conceptualized as due to the transfer function of the transduction process that results into an effective internal membrane potential, relative to the membrane's threshold. B: distance from threshold of the internal membrane potential is shown for the 3 frequencies outlined in A. This distance from threshold determines the amplitude of input noise necessary to observe an output from the receptor as shown by the C_1 -noise curves in A (double arrows in A and B show the corresponding distances to threshold). C: values taken from graph in A are replotted as a function of input frequency, for increasing input noise amplitudes. The inversion of the tuning curve at high-input noise is directly related to the threshold shifts illustrated in A and B. The dotted, dashed, and solid lines in C show the SNR values that would result in tuning curves from the corresponding lines illustrated (A). Compare this figure with A and D of Fig. 5.

terminated tuning curve. This frequency-dependent attenuation that determines the generator potential's distance from threshold is illustrated in Fig. 8B. This differential distance from threshold for each frequency contributes to the determination of the unit's response as input noise is superimposed. For frequencies to which the receptor is less sensitive (low and high frequencies in the example in Fig. 8C), i.e., when the generator potential is far below threshold, larger amplitude noise is required to reach threshold, causing C_1 to peak at larger input noise (Fig. 8A). The opposite is true for frequencies to which the neuron is preferentially sensitive. These differences in output SNR as a function of input noise across frequencies determine the changes in the shape of the tuning curve for different input noise levels (the correspondingly denoted lines in Fig. 8, A and C). The predicted tuning curve changes include the broadening of the tuning curve at midrange noise, and its inversion at high noise levels, as observed in our experiments (cf. Fig. 5, A and D, with Fig. 8, A and C).

This model does not consider other effects likely to be relevant when the input signal is increased to suprathreshold levels. As Fig. 5, D–F, shows, there is a systematic dependence of the maximum C_1 to the intensity of the input sine wave relative to the receptor threshold, at larger signal amplitudes. The details of this dependence could be grasped in numerical studies as suggested above. The precise mechano-electrical transfer function of a given receptor can be first determined and explicitly introduced in a numerical model to precisely elucidate the noise effects on tuning.

Conclusions

The changes in tuning curves with noise modulation reported here have strong implications regarding models of sensory perception. Contemporary models of sensory perception assume that the tuning properties of receptors determined in the absence of noise are preserved during everyday tasks. Our results show that this cannot be true. Therefore somatic information transmission through discrete independent channels is not tenable in a noisy environment, e.g., in everyday life. In fact, the tuning curves of these fibers at high noise levels should be more relevant to daily sensory experiences because sine-wave stimuli are never presented individually in the nonlaboratory environment. The results presented here for tactile sensory neurons have important similar implications for the other senses.

We thank A. Longtin, R. Durkovic, G. Gescheider, and J. P. Segundo for useful discussions and suggestions.

This research was funded by National Institute of Mental Health Grant MH-50064 and the Department of Neurosurgery at State University of New York, Syracuse.

Address for reprint requests: A. V. Apkarian, Neurosurgery Labs 766, Irving Ave., Syracuse, NY 13210.

Received 2 September 1997; accepted in final form 8 January 1998.

REFERENCES

- BELL, J., BOLANOWSKI, S., AND HOLMES, M. H. The structure and function of Pacinian corpuscles. *Prog. Neurobiol.* 42: 79–128, 1994.
- BENZI, R., SUTERA, A., AND VULPIANI, A. The mechanism of stochastic resonance. *J. Physics A* 14: L453–L457, 1981.
- BEZRUKOV, S. M. AND VODYANOV, I. Stochastic resonance in non-dynamical systems without response thresholds. *Nature* 385: 319–321, 1997.
- BOLANOWSKI, S. J., JR., GESCHIEDER, G. A., VERILLO, R. T., AND CHECHKOSKY, C. M. Four channels mediate the mechanical aspects of touch. *J. Acoust. Soc. Am.* 84: 1680–1694, 1988.
- BULSARA, A., JACOBS, E. W., ZHOU, T., MOSS, F., AND KISS, L. Stochastic resonance in a single neuron model: theory and analog simulation. *J. Theor. Biol.* 152: 531–555, 1991.
- BUÑO, W., JR., FUENTES, J., AND SEGUNDO J. P. Crayfish stretch-receptor organs: effects of length-steps with and without perturbations. *Biol. Cybern.* 31: 99–110, 1978.
- CHIALVO, D. R. AND APKARIAN, A. V. Modulated noisy biological dynamics: three examples. *J. Stat. Physics* 70: 375–391, 1993.
- CHIALVO, D. R., LONGTIN, A., AND MULLER-GERKING, J. Stochastic resonance in models of neuronal ensembles. *Phys. Rev. E* 55: 1798–1808, 1996.
- COLLINS, J. J., CHOW, C. C., AND IMHOFF, T. T. Stochastic resonance without tuning. *Nature* 376: 236–238, 1995.
- COLLINS, J. J., IMHOFF, T. T., AND GRIGG, P. Noise enhanced information transmission in rat SA1 cutaneous mechanoreceptors via aperiodic stochastic resonance. *J. Neurophysiol.* 76: 642–645, 1996.
- COLLINS, J. J., IMHOFF, T. T., AND GRIGG, P. Noise mediated enhancements and decrements in human tactile sensation. *Phys. Rev. E* 56: 923–926, 1997.
- DARIAN-SMITH, I. The sense of touch: performance and peripheral neural processes. In: *Handbook of Physiology. The Nervous System. Sensory Processes*. Washington, DC: Am. Physiol. Soc., 1985, sect. 1, vol. III, p. 739–788.
- DOUGLASS, J. K., WILKENS, L., PANTAZELOU, E., AND MOSS, F. Noise enhancement of information transfer in crayfish mechanoreceptors by stochastic resonance. *Nature* 365: 337–340, 1993.
- FAUVE, S. AND HESLOT, F. Stochastic resonance in a bistable system. *Phys. Lett.* 97A: 5–7, 1983.
- GAMMAITONI, L. Stochastic resonance and the dithering effect in threshold physical systems. *Phys. Rev. E* 52: 4691–4698, 1995.
- IKEDA, H. AND WRIGHT, M. J. The relationship between the “sustained-transient” and the “simple-complex” classifications of neurons in area 17 of the cat (Abstract). *J. Physiol. (Lond.)* 244: 58P–59P, 1975.
- JOHANSSON, R. S., LANDSTROM, U., AND LUNDSTROM, R. Responses of mechanoreceptive afferent units in the glabrous skin of the human hand to sinusoidal skin displacements. *Brain Res.* 244: 17–25, 1982.
- JOHNSON, K. O. Reconstruction of population response to a vibratory stimulus in quickly adapting mechanoreceptive afferent fiber population innervating glabrous skin of the monkey. *J. Neurophysiol.* 37: 48–72, 1974.
- LAMOTTE, R. H. AND MOUNTCASTLE, V. B. Capacities of humans and monkeys to discriminate between vibratory stimuli of different frequency and amplitude: a correlation between neural events and psychophysical measurements. *J. Neurophysiol.* 38: 539–559, 1975.
- LEEM, J. W., WILLIS, W. D., AND CHUNG, J. M. Cutaneous sensory receptors in the rat foot. *J. Neurophysiol.* 69: 1684–1699, 1993a.
- LEEM, J. W., WILLIS, W. D., WELLER, S. C., AND CHUNG, J. M. Differential activation and classification of cutaneous afferents in the rat. *J. Neurophysiol.* 70: 2411–2424, 1993b.
- LEVIN, J. E. AND MILLER, J. P. Broadband neural coding in the cricket sensory system enhanced by stochastic resonance. *Nature* 380: 165–168, 1996.
- LONGTIN, A., BULSARA, A., AND MOSS, F. Time-interval sequences in bistable systems and the noise-induced transmission of information by sensory neurons. *Phys. Rev. Lett.* 67: 656–659, 1991.
- MACADAR, O., WOLFE, G. E., O'LEARY, D. P., AND SEGUNDO, J. P. Response of the elasmobranch utricle to maintained spatial orientation, transitions and jitter. *Exp. Brain Res.* 22: 1–12, 1975.
- MAKOUS, J. C., FRIEDMAN, R. M., AND VIERCK, C. J., JR. A critical band filter in touch. *J. Neurosci.* 15: 2808–2818, 1995.
- MCNAMARA, B., WIESENFELD, K., AND ROY, R. Observation of stochastic resonance in a ring laser. *Phys. Rev. Lett.* 60: 2626–2629, 1988.
- MOUNTCASTLE, V. B., LAMOTTE, R. H., AND CARLI, G. Detection thresholds for stimuli in humans and monkeys: comparison with threshold events in mechanoreceptive afferent nerve fibers innervating the monkey hand. *J. Neurophysiol.* 35: 122–136, 1972.
- PANTAZELOU, E., MOSS, F., AND CHIALVO, D. Noise sampled signal trans-

- mission in an array of Schmitt triggers. In: *Noise in Physical Systems and $1/f$ Fluctuations*, edited by P. H. Handel and A. L. Chung. New York: Am. Inst. Physics, 1993, p. 549–552.
- PEI, X., WILKENS, A. L., AND MOSS, F. Light enhances hydrodynamic signaling in the multimodal caudal photoreceptor interneurons of the crayfish. *J. Neurophysiol.* 76: 3002–3011, 1996.
- SEGUNDO, J. P., VIBERT, J. F., PAKDAMAN, K., STIBER, M., AND MARTINEZ, O. D. Noise and the neurosciences: a long history, a recent revival, and some theory. In: *Origins: Brain and Self Organization*, edited by K. Pribram. Hillsdale, NJ: Erlbaum, 1994, p. 300–332.
- SIMONOTTO, E., RIANI, M., SEIFE, C., ROBERTS, M., TWITTY, J., AND MOSS, F. Visual perception of stochastic resonance. *Phys. Rev. Lett.* 78: 1186–1189, 1997.
- TALBOT, W. H., DARIAN-SMITH, I., KORNHUBER, H. H., AND MOUNTCASTLE, V. B. The sense of flutter-vibration: comparison of the human capacity with response patterns of mechanoreceptive afferents from the monkey hand. *J. Neurophysiol.* 31: 301–334, 1968.
- WATSON, A. B. AND PELLI, D. G. QUEST: a Bayesian adaptive psychometric method. *Percept. Psychophys.* 33: 113–120, 1983.
- WERNER, G. AND MOUNTCASTLE, V. B. Neuronal activity in mechanoreceptive cutaneous afferents: stimulus-response relations, Weber functions, and information transmission. *J. Neurophysiol.* 28: 359–397, 1965.
- WIESENFELD, K. AND MOSS, F. Stochastic resonance and the benefits of noise: from ice ages to crayfish and SQUIDS. *Nature* 373: 33–36, 1995.